Applied Physics Letters

# Suspended two-dimensional electron gases in $In_{0.75}Ga_{0.25}As$ quantum wells

Cite as: Appl. Phys. Lett. **116**, 232106 (2020); https://doi.org/10.1063/5.0013902
Submitted: 15 May 2020 . Accepted: 28 May 2020 . Published Online: 11 June 2020

C. Chen, S. N. Holmes, I. Farrer, H. E. Beere, and D. A. Ritchie

## ARTICLES YOU MAY BE INTERESTED IN

Two-dimensional electron gas at wurtzite–zinc-blende InP interfaces induced by modulation doping
Applied Physics Letters **116**, 232103 (2020); https://doi.org/10.1063/5.0009818

Strain suppressed Sn incorporation in GeSn epitaxially grown on Ge/Si(001) substrate
Applied Physics Letters **116**, 232101 (2020); https://doi.org/10.1063/5.0011842

Superconducting quantum many-body circuits for quantum simulation and computing
Applied Physics Letters **116**, 230501 (2020); https://doi.org/10.1063/5.0008202

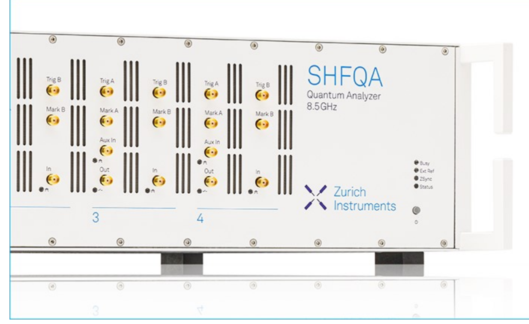

Learn how to perform the readout of up to 64 qubits in parallel
With the next generation of quantum analyzers on November 17th
Register now

© 2020 Author(s).

# Suspended two-dimensional electron gases in $In_{0.75}Ga_{0.25}As$ quantum wells

Cite as: Appl. Phys. Lett. **116**, 232106 (2020); doi: 10.1063/5.0013902
Submitted: 15 May 2020 · Accepted: 28 May 2020 ·
Published Online: 11 June 2020

View Online

Export Citation

CrossMark

C. Chen,[a] S. N. Holmes,[b] I. Farrer,[c] H. E. Beere, and D. A. Ritchie

AFFILIATIONS

Cavendish Laboratory, University of Cambridge, J. J. Thomson Avenue, Cambridge CB3 0HE, United Kingdom

[a]**Author to whom correspondence should be addressed:** cc638@cam.ac.uk
[b]**Present address:** London Centre for Nanotechnology, University College London, 17-19 Gordon Street, London WC1H 0AH, UK.
[c]**Present address:** Department of Electronic and Electrical Engineering, The University of Sheffield, Mappin Street, Sheffield S1 3JD, UK.

## ABSTRACT

We demonstrate that $In_{0.75}Ga_{0.25}As$ quantum wells can be freely suspended without losing electrical quality when the epitaxial strain-relieving buffer layer is removed. In applied magnetic fields, non-dissipative behavior is observed in the conductivity, and a current induced breakdown of the quantum Hall effect shows a lower critical current in the suspended layers due to efficient thermal isolation compared to the non-suspended-control device. Beyond the critical current, background impurity scattering in the suspended two-dimensional channel regions dominates with stochastic, resonant-like features in the conductivity. This device fabrication scheme offers the potential for thermally isolated devices containing suspension-asymmetry-induced, high spin–orbit coupling strengths with reduced electron–phonon interaction behavior but without introducing high levels of disorder in the processing.

*Published under license by AIP Publishing.* https://doi.org/10.1063/5.0013902

Suspended semiconductor structures with two-dimensional electron gases (2DEG) were envisaged and initially demonstrated as devices that could be thermally isolated from a temperature reservoir[1,2] and provide nanomechanical resonance functionality.[3,4] A thermally isolated structure would be important, for example, in thermal conductivity measurements,[5] where thermal shorting paths are unwanted features that reduce device performance. A suspended structure, which is thermally isolated from the substrate, is also essential to investigate the quenching of phonon-related transport properties that would allow a many body localized (MBL) ground state to be stabilized.[6] Depletion of charge at the edge of the device had beset these earlier studies[1,3] where the non-dissipative quantum Hall effect (QHE) was generally not observed at integer filling factors, i.e., with conductivity, $\sigma_{xx} \neq 0$ in the suspended regions of the device. This has been improved recently by changing the mesa shape and extending the suspension closer to the Ohmic contacts.[7]

InGaAs devices have a high spin–orbit coupling contribution to the electron dispersion as a result of the Rashba effect,[8] the size of which is dependent on the structural inversion asymmetry (SIA) of the confining potential. A compositionally graded InAlAs buffer is usually incorporated into these devices to reduce strain.[9–12] This buffer also allows the Al-rich composition to be etched away and the 2DEG to be released from the GaAs substrate. SIA should be sensitive to the removal of the buffer that could change the pinning strength at the chemically etched surface. In the QHE transport regime $\sigma_{xx} = 0$, the DC (direct current) current induced breakdown of the QHE can proceed via several processes with any heat instability more prevalent in the free-standing structures.

In this Letter, we discuss the electrical transport properties of freely suspended $In_{0.75}Ga_{0.25}As$ quantum wells (QWs) down to 400 mK. The clearly developed QHE in the suspended layer is studied during breakdown induced by a DC, and conclusions are made with further device development where sensitivity to heat dissipation or isolation from the substrate can be incorporated into a structure.

The sample contains a 30 nm wide $In_{0.75}Ga_{0.25}As$ QW. The details of the structure have been reported before.[12] The suspended membrane was released from the wafer using a HCl-based etchant ($3HCl: H_2O$)[13] that removes Al-rich InAlAs layers where the Al fraction is $>0.45$ in the graded buffer. 150 nm atomic layer deposition (ALD) $Al_2O_3$ was used as an etch mask and remained on the released membrane floating above the substrate. Control devices are fabricated at the same time from the same chip with the free-standing devices except for the final selective etching to release the membrane [see Figs. 1(a) and 1(b)]. A scanning electron microscopy (SEM) image of a free-standing Hall bar is shown in Fig. 1(c) with a 60° tilt from the vertical. As shown in the figure, the Hall bar is approximately 10 $\mu$m


Published under license by AIP Publishing

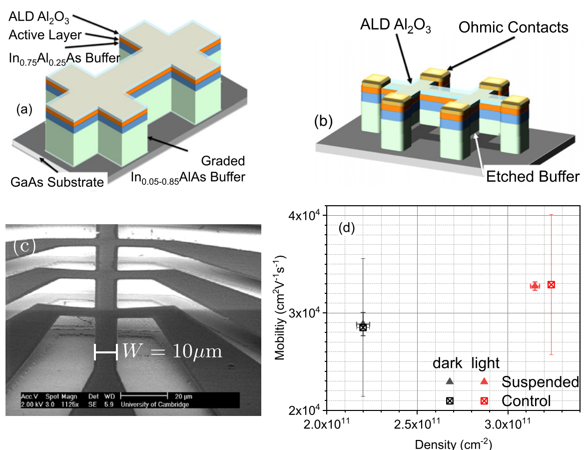


FIG. 1. (a) Hall bar and (b) suspended structure show that removing parting of the InAlAs graded buffer that is Al-rich (Al >0.45) releases the Hall bar with the QW from the GaAs substrate, while the Ohmic contacts are still on the substrate. (c) SEM image of a suspended device tilted 60° and the Hall bar channel width $W = 10\,\mu$m. (d) Mobility against carrier density in the suspended (filled triangles) and non-suspended-control (crossed squares) devices.

wide, and the voltage probes are partially suspended. This is very important as potential barriers between suspended and non-suspended parts of the membrane leads to partial scattering of the edge current channels, which will lead to non-zero longitudinal magneto-resistance at a high magnetic field.[7]

The transport properties of both the control and free-standing devices are characterized at 1.6 K and 400 mK both before and after *in situ* illumination with an infra-red light emitting diode. The density and mobility are summarized in Fig. 1(d). A total of three suspended and two non-suspended-control devices were measured with the experimental data presented in Fig. 2, which displays typical behavior. The photolithographic geometry of the Hall bar was used in the calculation of the mobility, and the values could be slightly underestimated due to side etching during the mesa definition. This also explains the large error bar on the control devices as the Hall bar width varies among devices. Both devices showed almost identical density and mobility after averaging both with and without illumination. This is in contrast to the situation with GaAs/AlGaAs structures where a reduction in mobility by a factor >2 is reported[7,14,15] in suspended structures.

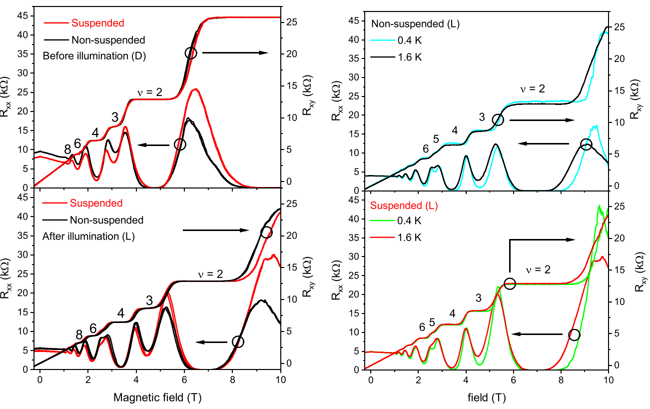


FIG. 2. Magnetoresistance $R_{xx}$ and $R_{xy}$ in the non-suspended-control and suspended devices before (D) and after illumination (L) at 1.6 K (left) and after illumination at 1.6 K and 400 mK (right).

Figure 2 shows the measured longitudinal and Hall resistances, $R_{xx}$ and $R_{xy}$, up to 10 T in the non-suspended-control and suspended devices before and after illumination at 1.6 K and the temperature dependence after illumination at 1.6 K and 400 mK. At low magnetic field (B), a positive change in resistivity, $\rho_{xx} = R_{xx}/(L/W)$, where $L$ is the length between the Ohmic contacts and $W$ is the width of the Hall bar, is seen. This is related to a weak localization effect rather than a spin–orbit-coupling-induced weak antilocalization effect. The conductivity correction at 0.1 T, $\Delta\sigma \approx e^2/h$ [obtained from a high magnetic field resolution measurement at a low field between ±0.1 T, where e is the fundamental charge and h is Planck's constant], is not further enhanced in the suspended layer in either magnitude or magnetic field dependence. There is no evidence of zero magnetic field spin-splitting due to Rashba spin–orbit coupling[8] in the suspended layer as the asymmetry of the confining potential is not significantly increased by the suspension process in this particular structure. This is partly due to the background impurities in the structure with only a small change in confining potential for the suspended layer that is verified by self-consistent simulation. It has been shown in previous transport measurements on similar but non-suspended structures[12,16] that the mobility in the $In_{0.75}Ga_{0.25}As$ QW is limited by background impurity scattering.

At high magnetic field, $R_{xx}$ manifests single frequency Shubnikov–de Haas oscillation with no beating and with clearly developed minima in $R_{xx}$ that goes to 0. This suggests that there is no scattering of edge states between suspended and non-suspended regions. The QHE is well defined, with plateaus at the quantized values of $R_{xy}$ at $h/\nu e^2$. The carrier density is the same in the suspended and non-suspended-control devices with no sign of parallel conduction, as the Hall effect carrier density agrees with that determined from the period of the Shubnikov–de Haas effect. There is a Zeeman splitting from 2.6 T (at Landau level filling factor $\nu = 5$) with $N_s = 3.1 \times 10^{11}$ cm$^{-2}$ that is reproduced in the suspended layer (see Fig. 2 after illumination). Neither of the devices displayed a temperature dependent magneto-transport behavior, i.e., changing density or mobility, apart from more clearer Zeeman splitting at 400 mK.

To inspect the difference in heat coupling to the substrate introduced by suspension, a DC ($I_{dc}$) was added to the nA AC excitation at filling factor $\nu = 2$ at 400 mK. The conductivity $\sigma_{xx}$, determined from the measured resistivity $\rho_{xx}$ and $\rho_{xy}$, is plotted against the DC in Fig. 3 as it represents the scattering along the length of the Hall bar. The conductivity rises above the experimental-zero background conductivity with increasing $I_{dc}$ and then increases up to a constant $\sigma_{xx}$. This is known as the breakdown of the QHE, and in the regime of the breakdown, the heat dissipation is in the source and drain Ohmic contact regions.[17] So, for both the suspended and non-suspended-control devices, the actual connection to the thermal reservoir is at the source and drain Ohmic contacts. This also explains why the resonant-like structure in $\sigma_{xx}$ is the same in both types of devices. This structure is independent of the direction and the rate that the current is swept (see multi-curves recorded with opposite sweep directions and different sweeping rates that are included in Fig. 3).


Published under license by AIP Publishing

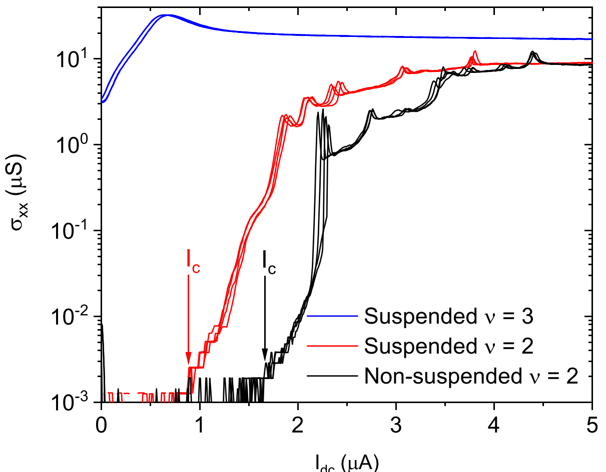


FIG. 3. Breakdown of the $\sigma_{xx} = 0$ state with increased DC $I_{dc}$ in the suspended ($\nu = 2, 3$) and non-suspended ($\nu = 2$) devices at 400 mK. The $\nu = 3$ state is dissipative and is shown for reference.

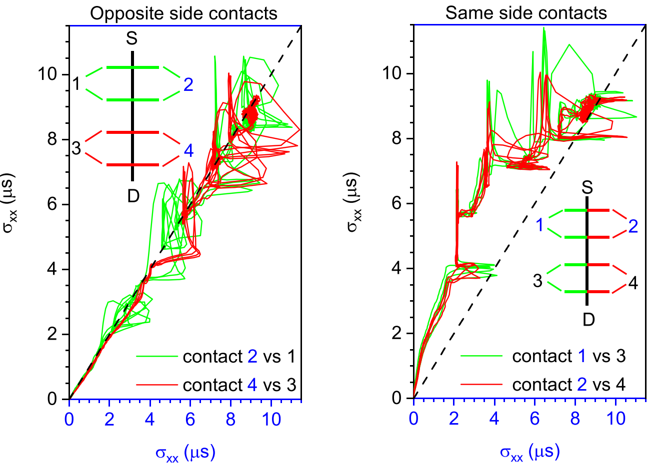


FIG. 4. Breakdown in $\sigma_{xx}$ with voltage probes on opposite sides (left) and the same side (right) of the device. S and D stand for source and drain contacts, respectively.

However, a difference in the critical current ($I_c$, labeled in Fig. 3) is observed at which $\sigma_{xx}$ > experimental zero conductivity that can be used as a measure of the thermal sensitivity of the device. The conductivity $\sigma_{xx}$ in the suspended device starts to increase at an $I_c$, which is a factor of ~2 less (0.9 $\mu$A compared to 1.7 $\mu$A in the non-suspended-control device). The critical current has been shown to depend logarithmically on the Hall bar width;[18] however, it is unlikely to be the variation in the Hall bar width, causing this difference measured here. This difference in critical current is more likely to be due to the reduction in volume of the devices, which has been reported as enhancing the sensitivity to heat dissipation processes.[1,7]

Figure 3 also shows the dependence of $\sigma_{xx}$ on $I_{dc}$ at filling factor $\nu = 3$. The $\nu = 3$ state is a Zeeman gap, and $\sigma_{xx}$ rises with $I_{dc}$ to the conductance peak, which would be there without Zeeman spin-splitting. The conductance is $\gtrsim 15$ $\mu$s when the QHE has broken down into the Ohmic behavior regime, well above the level of conductance where resonant-like features can be observed.

To understand the origin of the resonant-like structures, $\sigma_{xx}$ measured at voltage probes at opposite sides and the same side of the Hall bar is plotted against each other in Fig. 4. As stated previously, this structure is not sweep rate or sweep direction related. At low $\sigma_{xx}$ values $\leq 2$ $\mu$s, the opposite sides of the Hall bar have the same breakdown dependence with $I_{dc}$. However, there is a variation in the breakdown between contact combinations on the same side of the Hall bar. In other words, Fig. 4 shows an Ohmic contact combination symmetry for the breakdown behavior of $\sigma_{xx}$, which is characteristic of edge state transport.[19]

The resonant-like features beyond $I_c$ are stochastic and represent scattering events between the edge states (inter-Landau level scattering) as they interact with a bulk two-dimensional region that is known to have a high background impurity density in this channel material.[12,16] Thermally cycling the devices to 300 K and then recooling change the occurrence of the resonant-like features in $\sigma_{xx}$ due to the different background charge arrangements and the stochastic nature of the impurity scattering process. The resonant-like features in $\sigma_{xx}$ beyond the QHE breakdown are too narrow in the $I_{dc}$ range to be phonon related.[20] Further QHE breakdown mechanisms such as quasi-elastic inter-Landau level scattering have been modeled[21] to understand breakdown at $\nu = 2$ and 4. This mechanism operates in narrow channels and can be driven by emission of acoustic phonons or scattering with impurities. This process is likely to be weak here due to the wider Hall bar width of 10 $\mu$m that is much greater than the thermal phonon wavelength (1.2 $\mu$m at 300 mK) and the electron elastic mean free path (0.3 $\mu$m after illumination). Impurity scattering of the type dominant in InGaAs materials[12,16] can drive intraband phonon emission processes that lead to inelastic scattering between edge states in the breakdown of the QHE. This is more likely to be playing a role considering the importance of impurity scattering and the sensitivity of the suspended device to thermal transport processes.

In summary, freely suspended $In_{0.75}Ga_{0.25}As$ membranes can be fabricated with no reduction in mobility or carrier density. This technology can be applied to other combinations of semiconductor structures where thermal isolation is a prerequisite for device performance. The free standing devices show a higher sensitivity to heat dissipation with a DC induced heating. In particular, a reduction in the critical current for the breakdown of the non-dissipative QHE by a factor of ~2 is demonstrated in the suspended structures. Impurity scattering is important in this particular breakdown of the QHE and leads to stochastic, resonant-like structures in the conductivity before the onset of an Ohmic transport regime. In the GaAs/AlGaAs material system, a suspended one-dimensional channel showed an enhanced electron–electron interaction.[22] This is likely to be stronger in the InGaAs material system with Rashba spin–orbit coupling also playing a more significant role. Enhanced electron–electron interaction with thermal isolation from a heat reservoir is a partial requirement for the stabilization of a MBL ground state. To study the MBL state, controllable disorder has to be introduced by doping, for example, not by inhomogeneities in the device processing. The methodology reported here has


Published under license by AIP Publishing

demonstrated such a processing recipe and will provide devices for this research field.

This work was funded by EPSRC Grant Nos. EP/K004077/1 and EP/R029075/1, UK. We thank Professor Chris Ford for useful discussions.

## DATA AVAILABILITY

The data that support the findings of this study are available from the corresponding author upon reasonable request.

## REFERENCES

[1]R. H. Blick, F. G. Monzon, W. Wegscheider, M. Bichler, F. Stern, and M. L. Roukes, Phys. Rev. B **62**, 17103 (2000).
[2]M. Schmidt, G. Schneider, C. Heyn, A. Stemmann, and W. Hansen, Phys. Rev. B **85**, 075408 (2012).
[3]E. M. Höhberger, R. H. Blick, F. W. Beil, W. Wegscheider, M. Bichler, and J. P. Kotthaus, Physica E **12**, 487 (2002).
[4]Y. Zhang, Y. Watanabe, S. Hosono, N. Nagai, and K. Hirakawa, Appl. Phys. Lett. **108**, 163503 (2016).
[5]K. Schwab, E. A. Henriksen, J. M. Worlock, and M. L. Roukes, Nature **404**, 974 (2000).
[6]R. Nandkishore and D. A. Huse, Annu. Rev. Condens. Matter Phys. **6**, 15 (2015).
[7]A. G. Pogosov, M. V. Budantsev, E. Y. Zhdanov, D. A. Pokhabov, A. K. Bakarov, and A. I. Toropov, Appl. Phys. Lett. **100**, 181902 (2012).
[8]S. N. Holmes, P. J. Simmonds, H. E. Beere, F. Sfigakis, I. Farrer, D. A. Ritchie, and M. Pepper, J. Phys. **20**, 472207 (2008).
[9]S. M. Wang, C. Karlsson, N. Rorsman, M. Bergh, E. Olsson, T. G. Andersson, and H. Zirath, J. Cryst. Growth **175-176**, 1016 (1997).
[10]F. Capotondi, G. Biasiol, I. Vobornik, L. Sorba, F. Giazotto, A. Cavallini, and B. Fraboni, J. Vac. Sci. Technol., B **22**, 702 (2004).
[11]P. J. Simmonds, H. E. Beere, D. A. Ritchie, and S. N. Holmes, J. Appl. Phys. **102**, 083518 (2007).
[12]C. Chen, I. Farrer, S. N. Holmes, F. Sfigakis, M. P. Fletcher, H. E. Beere, and D. A. Ritchie, J. Cryst. Growth **425**, 70 (2015).
[13]N. J. Sauer and K. B. Chough, J. Electrochem. Soc. **139**, L10 (1992).
[14]S. J. Chorley, C. G. Smith, F. Perez-Martinez, J. Prance, P. Atkinson, D. A. Ritchie, and G. A. C. Jones, Microelectron. J. **39**, 314 (2008).
[15]E. M. Weig, R. H. Blick, T. Brandes, J. Kirschbaum, W. Wegscheider, M. Bichler, and J. P. Kotthaus, Phys. Rev. Lett. **92**, 046804 (2004).
[16]F. Capotondi, G. Biasiol, I. Vobornik, L. Sorba, F. Giazotto, A. Cavallini, and B. Fraboni, J. Cryst. Growth **278**, 538 (2005).
[17]U. Klaß, W. Dietsche, K. von Klitzing, and K. Ploog, Phys. B **169**, 363 (1991).
[18]N. Q. Balaban, U. Meirav, H. Shtrikman, and Y. Levinson, Phys. Rev. Lett. **71**, 1443 (1993).
[19]B. I. Halperin, Phys. Rev. B **25**, 2185 (1982).
[20]C. Chen, I. Farrer, S. N. Holmes, H. E. Beere, and D. A. Ritchie, J. Phys. **30**, 105705 (2018).
[21]L. Eaves and F. W. Sheard, Semicond. Sci. Technol. **1**, 346 (1986).
[22]A. A. Shevyrin, A. G. Pogosov, M. V. Budantsev, A. K. Bakarov, A. I. Toropov, S. V. Ishutkin, and E. V. Shesterikov, Appl. Phys. Lett. **104**, 203102 (2014).


Published under license by AIP Publishing